Sulfonated Poly(arylene ether sulfone)s with Phosphine Oxide Moieties: A Promising Material for Proton Exchange Membranes

Lingchao Fu, Guyu Xiao,* and Deyue Yan*

College of Chemistry and Chemical Engineering, State Key Laboratory of Metal Matrix Composites, Shanghai Jiao Tong University, 800 Dongchuan Road, Shanghai 200240, P. R. China

ABSTRACT Sulfonated poly(arylene ether sulfone)s with phosphine oxide moieties (sPESPO) were achieved by polycondensation of bis(4-hydroxyphenyl)phenylphosphine oxide with 3,3′-disulfonate-4,4′-difluorodiphenyl sulfone (SFDPS) and 4-fluorophenyl sulfone (FPSF). Sulfonated poly(arylene ether sulfone)s (sPES) were also synthesized by polymerization of 4,4′-sulfonyldiphenol with SFDPS and FPSF for comparison. The comparative study demonstrates that the sPESPO ionomers exhibit strong intermolecular interactions and high oxidative stability because of the phosphine oxide groups. Furthermore, the sPESPO membrane and the sPES membrane with an equal ion exchange capacity show much different nanophase separation morphology. As a result, the former shows better properties than the latter. The sPESPO membranes exhibit excellent overall properties. For instance, the sPESPO membrane, with a disulfonation degree of 45%, exhibits high thermal and oxidative stability. Moreover, it shows a water uptake of 30.8% and a swelling ratio of 15.8% as well as a proton conductivity of 0.087 S/cm at 80 °C.

KEYWORDS: phosphine oxide • poly(arylene ether sulfone)s • proton exchange membrane • sulfonated

INTRODUCTION

Proton exchange membrane fuel cells (PEMFC) are one of green power sources, which convert chemical energy directly into electrical energy with high energy conversion efficiency, low emission of pollutants, and low operating temperature (1). Proton exchange membranes (PEMs) are a key component of PEMFC. Nafion perfluorinated membrane is now the reference membrane for PEMs. However, it exhibits technical limitations such as low conductivity at elevated temperatures or low humidity, high methanol crossover, and high cost, hindering its extensive applications in PEMFC (2). Therefore, the exploration of modified perfluorinated PEMs (3−5), partially fluorinated PEMs (2, 6, 7), and alternative aromatic PEMs (1, 2, 8−14) is attracting worldwide attention.

High-performance polymers are of interest as the matrix of PEMs because of their high mechanical properties and thermal stability as well as chemical stability (1). As a typical route, the sulfonic acid groups were attached to the backbone to produce the corresponding ionomers for PEMs (1). Among them, sulfonated poly(arylene ether sulfone)s (15−17), poly(arylene ether ketone)s (18−20), poly(arylene thioether)s (21, 22), polyimides (23−25), polyphosphazenes (26, 27), polybenzimidazoles (28−31), polybenzothiazoles (32), poly(arylene ether/thioether phosphine oxide)s (33−38), and their derivatives (39−41) have been investigated extensively as PEM materials. Sulfonated poly(arylene ether/thioether phosphine oxide)s are particularly interesting as PEMs because the strong polar phosphine oxide moieties show high water retention and excellent adhesive ability with other polymers and inorganic materials (33−38). These ionomers thus showed advantages at high temperatures or low humidity. Moreover, they are also favorable for preparing composite PEMs by blending with other polymers or by doping with inorganic materials. However, these sulfonated poly(arylene ether/thioether)s with phosphine oxide moieties were synthesized by polycondensation of sulfonated bis(4-fluorodiphenyl)phenyl phosphine oxide and bis(4-fluorophenyl)phenyl phosphine oxide with dihydroxyl monomers or dimercapto monomers. In other words, the phosphine oxide moieties of products derive from the monomers of sulfonated bis(4-fluorodiphenyl)phenyl phosphine oxide and bis(4-fluorophenyl)phenyl phosphine oxide.

In this article, bis(4-hydroxyphenyl)phenylphosphine oxide (BHPPO) was synthesized at first, then sulfonated poly(arylene ether sulfone)s with phosphine oxide moieties (sPESPO) were synthesized by polycondensation of BHPPO with 3,3′-disulfonate-4,4′-difluorodiphenyl sulfone (SFDPS) and 4-fluorophenyl sulfone (FPSF). In this case, the phosphine oxide moieties of resulting polymers derive from the dihydroxyl monomer of BHPPO. The incorporation of phosphine oxide moieties was expected to make the products possess strong water retention as well as intermolecular interactions, and then to improve their overall properties. For comparison purposes, sulfonated poly(arylene ether sulfone)s (sPES), with a disulfonation degree of 40%, were also synthesized by polymerization of 4,4′-sulfonyldiphenol with SFDPS and FPSF. The structure of resulting ionomers was characterized, and the property differences between

* Corresponding author. E-mail: gyxiao@sjtu.edu.cn; dyyan@sjtu.edu.cn.
Received for review January 27, 2010 and accepted May 17, 2010

DOI: 10.1021/am1000739

sPESPO and sPES were investigated in detail so as to determine whether they are a promising material for PEMs or not.

EXPERIMENTAL SECTION

Materials. Phenylphosphonic dichloride was purchased from Aldrich and used as received. 4-Bromoanisole and Magnesium powder were obtained from Shanghai Chemical Reagent Co. and used without further purification. 4-Fluorophenyl sulfone (FPSF) and 4,4′-sulfonyldiphenol (SFDP) were purchased from Aldrich. FPSF was purified by recrystallization with ethanol while SFDP was recrystallized from methanol/H_2O before use. *N*,*N*-Dimethylacetamide (DMAc) was dehydrated by calcium hydride for 24 h and then distilled under reduced pressure. Tetrahydrofuran (THF) was dehydrated with filamentous sodium and distilled prior to use. Toluene was distilled prior to use. Other chemicals and solvents were obtained from commercial sources and used without further purification. 3,3′-Disulfonate-4,4′-difluorodiphenyl sulfone (SFDPS) was synthesized according to our previous report (42). Bis(4-hydroxyphenyl)phenylphosphine oxide (BHPPO) was synthesized in our laboratory by a modified procedure (43, 44) (see the Supporting Information).

Synthesis of Polymers. As a typical example, the preparation procedure of sPESPO with a disulfonation degree of 40% was described as follows. 0.9309 g (0.003 mol) of BHPPO, 0.5500 g (0.0012 mol) of SFDPS, 0.4577 g (0.0018 mol) of FPSF, 0.4561 g (0.0033 mol) of K_2CO_3, 8 mL of DMAc, and 8 mL of toluene were added into a 100 mL three-necked round-bottom flask with a mechanical stirrer, a condenser, a Dean−Stark trap, and a nitrogen inlet/outlet. The reaction mixture was stirred at room temperature for 0.5 h to dissolve the reactants and then heated to 160 °C for 4 h to dehydrate the system. Subsequently, the reaction mixture was heated to 165 °C. After removing toluene, the reaction was held at 165 °C for 3 days until the product became very viscous. The reaction mixture was diluted with 2 mL of DMAc after being cooled to 110 °C and then poured into deionized water with vigorous stirring. The fibrous product was immersed in hot deionized water to remove inorganic salts. The resulting polymer was dried under a vacuum at 100 °C for 48 h.

Yield: 97%. ^{1}H NMR (DMSO-d_6, ppm): 8.37−8.30, 8.00−7.92, 7.92−7.80, 7.72−7.58, 7.58−7.48, 7.30−7.18, 7.18−7.05. ^{13}C NMR (DMSO-d_6, ppm): 160.623, 158.799, 157.492, 140.679, 136.833, 136.088, 134.759 (d, J_{cp} = 10.7 Hz), 134.416, 133.140 (d, J_{cp} = 103.3 Hz), 132.851, 132.167 (d, J_{cp} = 9.1 Hz), 130.738, 129.499 (d, J_{cp} = 10.6 Hz), 129.028 (d, J_{cp} = 104.9 Hz), 129.005, 121.982, 120.287 (d, J_{cp} = 10.6 Hz), 120.021.

Preparation of Membranes. The salt form sPESPO was dissolved in NMP at a concentration of 6% (w/v). The obtained solution was cast to a dust-free glass plate and dried at 70 °C for 48 h. After being cooled to room temperature, the glass plate was immersed in deionized water and the membranes peeled off. The membrane was converted to the acid form by soaking in 0.5 M H_2SO_4 at 90 °C for 2 h and then in deionized water at 90 °C for 2 h according to a similar procedure (45).

Measurements. ^{1}H and ^{13}C NMR spectra were recorded on a Varian MERCURY 173 plus 400 MHz spectrometer using deuterated dimethyl sulfoxide (DMSO-d_6) as solvent and tetramethylsilane (TMS) as internal standard. Fourier transformation infrared (FT-IR) spectra were performed on a Bruker Equinox-55 Fourier transform spectrometer. A series of thin membranes were used as the samples for FT-IR. The molecular weight and polydispersity index of polymers were measured on a PE Series 200 gel permeation chromatography (GPC) equipped with a refractive index detector, using *N*,*N*-dimethylformamide (DMF) containing 0.05 mol/L of LiBr as eluant. Polystyrene standards were used for calibration. The thermal degradation was investigated on a Q5000 IR TA thermogravimetric analyzer (TGA) in air from 150 to 700 at 20 °C/min. The samples in the acid form were kept at 150 °C for 30 min to remove moisture. The differential thermal analysis (DSC) was conducted on a PE Pyris-1 differential scanning calorimeter. The DSC samples in the acid form were also preheated at 150 °C for 30 min for removal of absorbed water. The temperature then decreased to 80 at 5 °C/min. The DSC curves were recorded in a range of 80−350 °C at a heating rate of 10 °C/min.

The ion exchange capacity (IEC) of ionomer membranes were measured by titration. The H^+ within the acid form membranes was exchanged by Na^+ after immersing in saturated NaCl solution for 48 h, and the released H^+ was titrated by 0.01 M NaOH solution with phenolphthalein as an indicator. The IEC of membranes thus could be obtained.

The water uptake and swelling were determined as follows. The acid form membranes were dried in vacuo at 100 °C for 24 h and measured the weight and length of the dry membranes. Subsequently, the dry membranes were soaked in deionized water at given temperatures for an interval of 24 h. After wiping off the water on the surface, the weight and length of the wet membranes were recorded. The measurement process should be performed as quickly as possible in order to reduce the error. The water uptake and swelling of membranes were calculated by the following equations

$$\text{water uptake} = (W_{wet} - W_{dry})/W_{dry} \times 100\%,$$
$$\text{swelling} = (L_{wet} - L_{dry})/L_{dry} \times 100\%$$

where W_{wet} and W_{dry} are the weight of the wet and dry membranes, L_{wet} and L_{dry} are the length of the wet and dry membranes, respectively.

The testing of oxidative stability for membranes was performed according to a typical procedure (24). The membrane samples (0.5 cm ×1 cm) with a thickness about 40 μm were tested in Fenton's reagent (30% H_2O_2 containing 30 ppm $FeSO_4$) at room temperature. The oxidative stability was evaluated by the elapsed time when the membrane started to dissolve (τ_1) and dissolved completely (τ_2) like the previous report (24).

The longitudinal proton conductivity of membranes was measured by a Solartron Analytical SI 1287 electrochemical test system over the frequency range from 1 M Hz to 1 Hz following the previous route (34, 35). The acid form membranes for testing were immersed in ultrapure water for 24 h to remove the residual acid, and then washed with ultrapure water. The proton conductivity (σ) was obtained according to the formula of $\sigma = L/(RWd)$, where L is the distance between two electrodes, whereas R, W, and d are the resistance, the width, and the thickness of samples, respectively.

The microstucture of membranes were determined by atomic force microscopic (AFM) with a Digital Instrument Nano Scope III in tapping mode. The membrane samples were obtained as following: the acid form polymers were dissolved in NMP, then cast to the glass plates (1 cm ×1 cm) and heated to vaporize the solvent. All samples were measured under ambient conditions (40% relative humidity).

RESULTS AND DISCUSSION

Synthesis of Polymers. The homopolymers, poly(arylene ether sulfone)s with phosphine oxide moieties (PESPO), were synthesized by polycondensation of bis(4-hydroxyphenyl)phenylphosphine oxide (BHPPO) and 4-fluorophenyl sulfone (FPSF), while sulfonated poly(arylene ether sulfone)s with phosphine oxide moieties (sPESPO-xx) were obtained by polymerization of BHPPO with 3,3′-disulfonate-

Scheme 1. Synthesis of sPES-40, PESPO, and the sPESPO Series Polymers

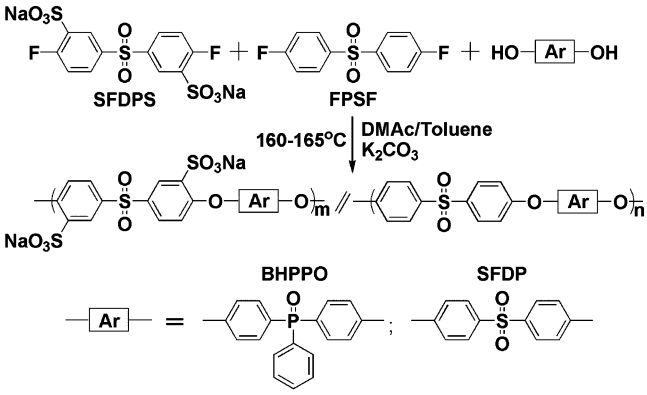

4,4′-difluorodiphenyl sulfone (SFDPS) and FPSF, the "xx" of which is the molar percent ratio of SFDPS in the difluorinated monomers. For comparison, sulfonated poly(arylene ether sulfone)s with a disulfonation degree of 40% (sPES-40) were also prepared by polycondensation of 4,4′-sulfonyldiphenol (SFDP) with SFDPS and FPSF. The reaction routes are shown in Scheme 1. DMAc was used as the solvent and toluene was used as the azeotropic dehydrating agent. The sulfonation degree of sPESPO was determined by adjusting the ratio of SFDPS to FPSF. The feed ratios and results of polycondensation reaction are exhibited in Table 1. As shown, the molecular weight of products is higher than 3.7×10^4 g/mol, and the polydispersity index (PDI) is in a range of 1.36−1.57, which is low for the step-growth polymers. As mentioned above, the resulting polymers were immersed in hot water to remove inorganic salts, thus the low-molecular-weight part was removed inevitably. This prompted the products to show low PDI. Similarly, the sulfonated poly(arylene thioether)s with low PDI were observed in the previous report (41). The resulting polymers all could form transparent, flexible, and tough membranes, further indicating that they have high molecular weight.

As a typical example, the ^{13}C and dept135 NMR spectra of sPESPO-40 are exhibited in Figure 1. The dept135 NMR spectrum, showing only the signal of odd-carbon atoms, was used to analyze the ^{13}C NMR spectrum of sPESPO-40. As shown, all signal peaks of carbon atoms were well assigned. Carbons 8−13 in sPESPO-40 exhibited a double splitting peak because of the coupling of C/P. Carbons 10 and 11 showed a coupling constant J_{cp} of 103−105 Hz. In contrast,

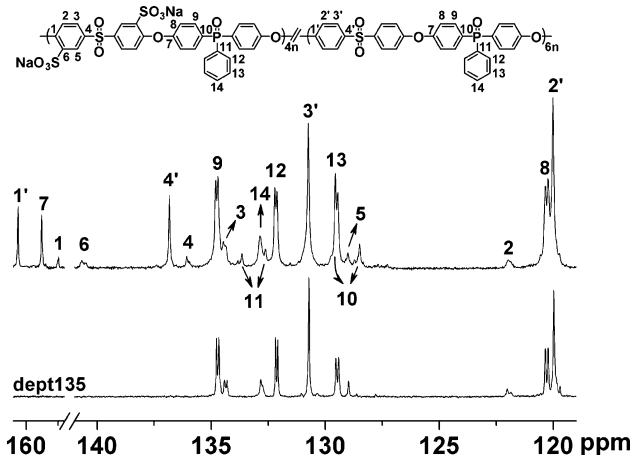

FIGURE 1. ^{13}C and dept135 NMR spectra of sPESPO-40.

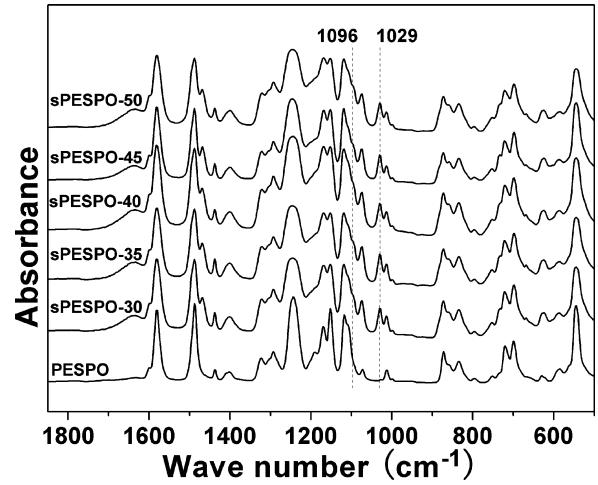

FIGURE 2. FT-IR spectra of PESPO and the sPESPO series.

carbons 8, 9, 12, or 13 displayed only a coupling constant J_{cp} of about 10 Hz. The ^{13}C and dept135 NMR spectra of sPESPO-40 confirmed its chemical structure.

The IR spectra of PESPO and the sPESPO series are exhibited in Figure 2. As shown, PESPO and the sPESPO series all displayed an absorption band at 1169 cm^{-1}, attributed to the characteristic stretching vibration of phosphine oxide groups (36−38). Different from PESPO, the sPESPO series membranes indicated a characteristic absorption at 1029 cm^{-1}, which are ascribed to the symmetric stretching vibrations of $-SO_2-$ in sulfonate groups. In addition, the sPESPO series also showed a shoulder band at

Table 1. Feed Ratios and Results of Polycondensation Reaction

			GPC			
polymer	SFDPS/FPSF	BHPPO/SFDP	$M_n \times 10^{-4}$	$M_w \times 10^{-4}$	PDI	yield (%)
	(molar ratio)					
PESPO	0/100	100/0	4.18	6.58	1.57	95
sPESPO-30	30/70	100/0	4.57	6.86	1.50	98
sPESPO-35	35/65	100/0	3.76	5.73	1.53	97
sPESPO-40	40/60	100/0	6.10	8.58	1.41	96
sPESPO-45	45/55	100/0	4.80	6.94	1.45	98
sPESPO-50	50/50	100/0	4.00	5.52	1.38	96
sPES-40	40/60	0/100	5.94	8.11	1.36	98

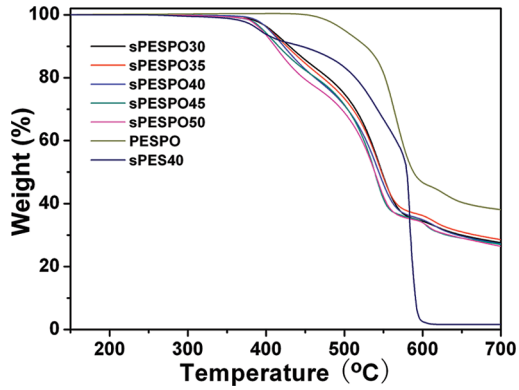

FIGURE 3. TGA traces of sPES-40, PESPO, and the sPESPO series.

Table 2. T_{d5}, IEC, and Oxidative Stability of Polymer Membranes

		IEC (meq/g)			
polymer	T_{d5} (°C)	calcd	measd	τ_1[a] (h)	τ_2[a] (h)
PESPO	500				
sPESPO-30	407	1.05	0.98	50	68
sPESPO-35	406	1.21	1.13	48	66
sPESPO-40	405	1.36	1.30	48	63
sPESPO-45	397	1.51	1.44	46	60
sPESPO-50	395	1.65	1.57	42	54
sPES-40	392	1.51	1.42	5	14

[a] τ_1 and τ_2 refer to the elapsed time when the membranes start to dissolve and are dissolved completely, respectively.

1096 cm^{-1}, arising from the asymmetric stretching vibrations of the sulfone groups in $-SO_3Na$. Other sulfonated polymers also indicated similar absorption bands arising from sulfonate groups (24, 36). Hence the IR spectra of PESPO and the sPESPO series further confirmed their chemical structure.

Thermal Properties of Polymers. The TGA curves of resulting polymers in air are displayed in Figure 3. As shown, the homopolymer PESPO has only one weight loss at ~550 °C, which is attributed to the degradation of polymer backbone. In contrast, the sPESPO series and sPES-40 exhibited two weight loss in their TGA curves. The first weight loss started at about 390 °C is due to desulfonation, whereas the second one at around 520 °C is ascribed to the degradation of polymer backbone. The 5% weight-loss temperature (T_{d5}) is listed in Table 2. As observed from Table 2, the homopolymer PESPO showed a T_{d5} of 500 °C, whereas the sPESPO series indicated a T_{d5} of 395−407 °C, which is much lower than that of PESPO. Moreover, the T_{d5} of sPESPO series decreased with increasing sulfonation degree. These phenomena are because the first weight loss of sPESPO series results from desulfonation, similar to other sulfonated polymers (24, 45). Additionally, sPESPO-45 showed a T_{d5} of 397 °C, higher than that of sPES-40 with an equal IEC.

On the other hand, all the products exhibited no exothermal/endothermal peak and no glass transition in the DSC curves at the temperatures of 80−350 °C. The absence of T_g is probably due to the fact that the bulky pendant groups and strong intermolecular interactions hinder the movement of molecular segments (36).

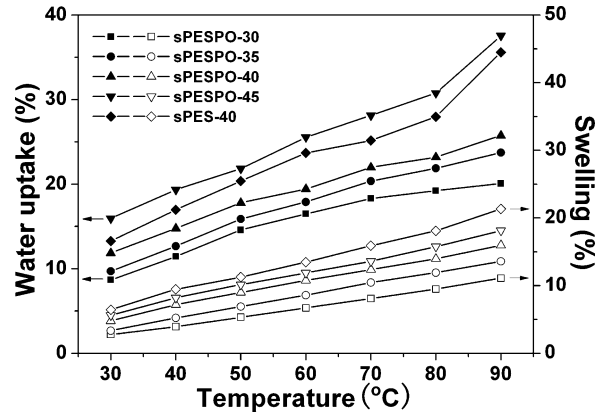

FIGURE 4. Water uptake and swelling of membranes at various temperatures.

Ion Exchange Capacity, Water Uptake, and Swelling. The theoretic ion exchange capacity (IEC) of sulfonated polymers could be calculated by their molecular formulas, while the experimental value of IEC was measured by titration (38). The values of IEC are compiled in Table 2. The experimental IEC values are in the range of 0.98−1.57 meq/g, which basically coincide with the calculated ones. The errors between the experimental and theoretical IEC are 5−7%, less than some of the reported values (23). This result indicates that the sulfonic acid groups were successfully attached to the polymer backbone by polycondensation.

The water uptake and swelling are two important parameters for PEMs, which represent their water retention and dimensional stability, respectively. According to the vehicle mechanism of proton transport, an appropriate amount of water content in PEMs is necessary for achieving high proton conductivity (9, 32). On the other hand, excessive water content in membranes could deteriorate dimensional stability and even results in serious loss of mechanical properties (9). Therefore, a promising PEM should balance the two properties and thus achieved high proton conductivity as well as excellent dimensional stability. The water uptake and swelling were measured at the temperatures ranging from 30 to 90 °C. The results are displayed in Figure 4. As shown, for the sPESPO series membranes, the water uptake increased with sulfonation degree and temperature. Of all the membranes, the sPESPO-45 membrane showed the highest water uptake in the entire temperature region, but it displayed a water uptake of only 30.8% at 80 °C, very close to that (30%) of Nafion 117 (35). As mentioned above, sPESPO-45 and sPES-40 have an equal IEC, the former, however, exhibited higher water uptake than the latter in the whole temperature region. This might be because of the high water retention of phosphine oxide moieties, as observed in our previous report (46). In addition, the water uptake and swelling of the sPESPO-50 membrane was absent in Figure 4 because it swelled excessively and lost most mechanical strength in the course of the above-mentioned acidification process.

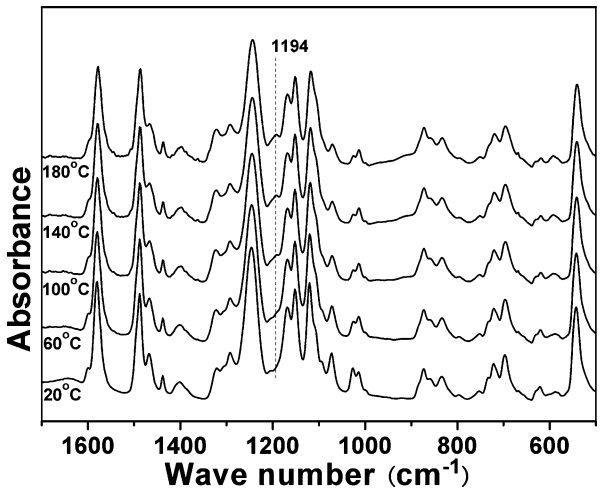

FIGURE 5. FT-IR spectra of the acid form sPESPO-45 membrane at various temperatures.

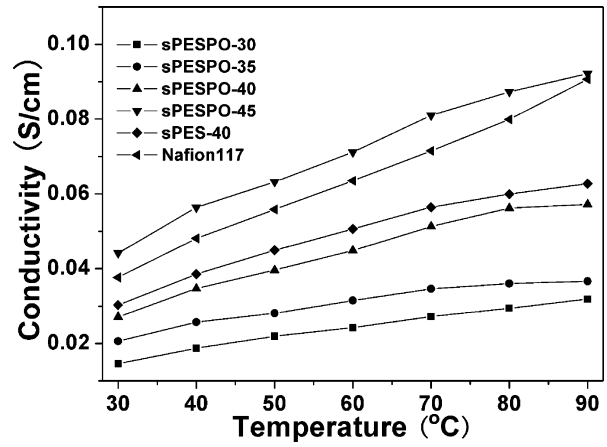

FIGURE 6. Proton conductivity of membranes at various temperatures (100% RH).

The swelling as functions of temperature and sulfonation degree is also displayed in Figure 4. It could be found that the curve profile of swelling is similar to that of water uptake. The swelling increased with sulfonation degree and temperature. Among the sPESPO series membranes, the sPESPO-45 membrane showed the highest swelling in the entire temperature region, but it only exhibited a swelling of 15.8% at 80 °C, lower than that (20%) of Nafion 117 (35). In addition, the sPESPO-45 membrane, however, displayed lower swelling than the sPES-40 membrane, although the former has higher water uptake than the latter. This might arise from the strong polar phosphine oxide groups of sPESPO-45 (46), which will be discussed in the next part. In conclusion, sPESPO-45 showed higher water uptake as well as better dimensional stability than sPES-40 with an equal IEC.

Intermolecular Interactions. The intermolecular interactions play an important role in the swelling of PEMs (41). It is well-known that the phosphine oxide groups show a dipole moment of 9.0×10^{-30} C.m (34). This high dipole moment provides the sPESPO membranes with strong dipole force, beneficial for lowering the swelling. On the other hand, the hydrogen bonds between the phosphine oxide and sulfonic acid groups also could limit the swelling, which are always confirmed by variable temperature FT-IR spectroscopy. The FT-IR spectra of sPESPO-45 membrane (in the acid form) as a function of temperature are shown in Figure 5. As shown, the sPESPO-45 membrane exhibited a strong characteristic absorption at 1169 cm^{-1}, assigned to the stretching vibration of phosphine oxide groups. However, it displayed no absorption band at 1194 cm^{-1} at room temperature but showed an obvious band at 1194 cm^{-1} at elevated temperatures. Moreover, its intensity enhanced with increasing temperature. The characteristic peak at 1194 cm^{-1} is attributed to the "free" phosphine oxide groups. Therefore, these results revealed that the H-bonded phosphine oxide groups partly dissociated into "free" phosphine oxide groups at elevated temperatures, that is to say, there are hydrogen bonds between the phosphine oxide and sulfonic acid groups in the sPESPO membranes. The intermolecular hydrogen bonds are favorable to depress the swelling of sPESPO membranes. As a result, though sPESPO-45 exhibited higher water uptake than sPES-40, the former still showed lower swelling than the latter.

Proton Conductivity. The ionomer membranes were fully hydrated by immersion in ultrapure water for 48 h before measuring their proton conductivity. The proton conductivity of sPES-40 and sPESPO membranes is shown in Figure 6. For comparison, the proton conductivity of Nafion 117 was also measured, which is comparable to the reported value (20, 32). As expected, for the sPESPO series membranes, the proton conductivity increased with increasing temperature and sulfonation degree. The sPESPO-45 membrane displayed the highest proton conductivity in the whole temperature region. It denoted a proton conductivity of 0.087 S/cm at 80 °C, higher than that of Nafion 117 under the same conditions. Other sPESPO membranes all showed proton conductivity lower than that of Nafion 117. Interestingly, the sPESPO-45 membrane showed much higher proton conductivity than the sPES-40 membrane with an equal IEC, partially because of its higher water uptake than sPES-40. In addition, their microstructure might also be a reason.

Oxidative Stability. Up to now, the longest lifetime of aromatic PEMs is only 5,000 h, still lower than that of Nafion (12, 47). Hence the oxidative stability of aromatic PEMs is especially significant for fuel cell applications. According to a well-established procedure (23, 24), the oxidative stability of sPES-40 and sPESPO membranes was evaluated by recording the elapsed time when the membrane samples started to dissolve (τ_1) and dissolved completely (τ_2) in Fenton's reagent (30% H_2O_2 containing 30 ppm $FeSO_4$) at room temperature. The elapsed time (τ_1 and τ_2) are collected in Table 2. As shown, the τ_1 and τ_2 for the sPESPO membranes are much higher than those of other aromatic PEMs (23, 24), respectively, indicating high oxidative stability. Moreover, τ_1 and τ_2 decreased with increasing sulfonation degree, that is to say, the oxidative stability of sPESPO membranes dropped with increasing sulfonation degree, similar to the previous reports (23, 24, 32). In contrast, the τ_1 and τ_2 of the sPES-40 membrane are 5 and

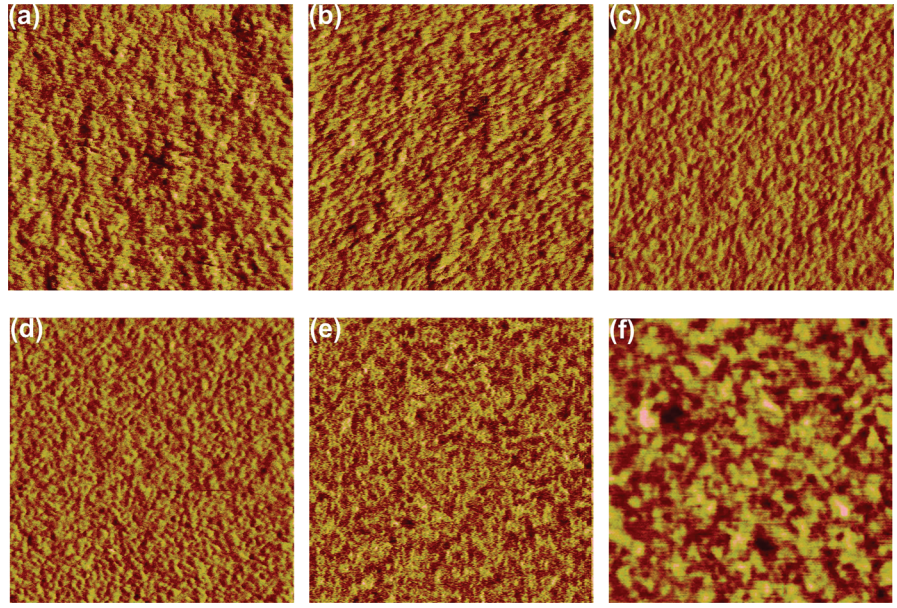

FIGURE 7. AFM phase images (500 nm × 500 nm) of membranes: (a) sPESPO-30, (b) sPESPO-35, (c) sPESPO-40, (d) sPESPO-45, (e) sPESPO-50, and (f) sPES-40.

14 h, much lower than those of the sPESPO-45 membrane, respectively. This illustrated that the sPESPO-45 membrane exhibited much better oxidative stability than the sPES-40 membrane. A tentative explanation is as follows. In the solution of Fenton's reagent, the ferrous ions catalyze H_2O_2 to produce hydroperoxy radicals and they attack the membranes and cause the decomposition (48). However, the phosphine oxide groups of sPESPO membranes chelate the ferrous ions in Fenton's reagent and passivate the radicals, similar to the earlier reports (49, 50). These effects depressed the oxidative degradation and endowed sPESPO-45 with high oxidative stability. In addition, as a reference, the oxidative stability of Nafion 117 was also investigated. It showed no recognizable change after treatment for 50 h like the previous report (24).

Microstucture of Membranes. The microstructure of PEMs greatly affects their macroscopic properties such as water uptake, swelling, and proton conductivity (9, 32). The microstructure of sPES-40 and sPESPO membranes was investigated by AFM in tapping mode. The AFM phase images were recorded on a 500 × 500 nm^2 size scale and exhibited in Figure 7. As shown, all the samples showed nanophase separation morphology as indicated by the dark and bright regions. The dark regions are ascribed to the hydrophilic ionic domains containing a small amount of water, while the bright regions are composed of the hydrophobic backbone (36, 45). The hydrophilic ionic domains are responsible for water uptake and proton transport, whereas the hydrophobic domains provide the membrane with mechanical strength and prevent it from swelling excessively in water (9, 32). For most aromatic PEMs, both the connectivity and size of ionic domains increase obviously with increasing sulfonation degree, so these PEMs with high IEC show well-connected and large ionic domains (32, 51). As a result, they generally suffered excessive swelling or even lost most mechanical strength at high IEC (9, 32). As shown in Figure 7, the sPESPO-30−45 membranes exhibit nanophase separated images, where the connectivity of ionic domains slightly increase but their size even show a slight decrease with sulfonation degree like the previous reports (51, 52). The increased connectivity of ionic domains could improve the water uptake and proton conductivity (52−54). Therefore, their water uptake and proton conductivity enhanced with sulfonation degree. From sPESPO-45 to sPESPO-50, the AFM phase images presented great change, indicating that the sPESPO membranes reach a percolation limit at a disulfonation degree of 50%. This change might lead to the result that sPESPO-45 still showed low swelling, whereas sPESPO-50 swelled excessively at elevated temperature, a similar phenomenon as was reported previously (51).

On the other hand, though the sPES-40 and sPESPO-45 membranes have an equal IEC, they exhibited much different AFM phase images, because of their different molecular structure. This factor might cause the former to display lower proton conductivity than the latter, similar to the earlier study (53, 54).

CONCLUSIONS

Sulfonated poly(arylene ether sulfone)s with phosphine oxide moieties (sPESPO) were synthesized by polycondensation of bis(4-hydroxyphenyl)phenylphosphine oxide with 3,3′-disulfonate-4,4′-difluorodiphenyl sulfone (SFDPS) and 4-fluorophenyl sulfone (FPSF). For comparison purposes, sulfonated poly(arylene ether sulfone)s with a disulfonation degree of 40% (sPES-40) were also prepared by polymerization of 4,4′-sulfonyldiphenol with SFDPS and FPSF. In contrast to sPES-40, the sPESPO ionomers exhibited strong intermolecular interactions and high oxidative stability because of the phosphine oxide groups. Moreover, the sPESPO-45 membrane and the sPES-40 membrane with an equal IEC showed much different nanophase separation morphology. As a result, the former showed higher proton conductivity,

and lower swelling in comparison with the latter. The sPESPO membranes exhibited excellent overall properties. For instance, the sPESPO-45 membrane exhibited high thermal and oxidative stability. Moreover, it showed a water uptake of 30.8% and a proton conductivity of 0.087 S/cm as well as a swelling of 15.8% at 80 °C.

Acknowledgment. This research was supported by the National Natural Science Foundation of China (50633010 and 50973061), the National Basic Research Program (2007CB808000 and 2009CB930400), and the Shanghai Leading Academic Discipline Project (B202).

Supporting Information Available: Synthesis of bis(4-hydroxyphenyl)phenylphosphine oxide (BHPPO) and its ^{13}C and dept135 NMR spectra (PDF). This material is available free of charge via the Internet at http://pubs.acs.org.

REFERENCES AND NOTES

(1) Li, Q. F.; Jensen, J. O.; Savinell, R. F.; Bjerrum, N. J. *Prog. Polym. Sci.* **2009**, *34*, 449–477.
(2) Savadogo, O. *J. Power Sources* **2004**, *127*, 135–161.
(3) Subianto, S.; Mistry, M. K.; Choudhury, N. R.; Dutta, N. K.; Knott, R. *ACS Appl. Mater. Interfaces* **2009**, *1* (6), 1173–1182.
(4) Xu, K.; Chanthad, C.; Gadinski, M. R.; Hickner, M. A.; Wang, Q. *ACS Appl. Mater. Interfaces* **2009**, *1* (11), 2573–2579.
(5) Lin, J.; Wycisk, R.; Pintauro, P. N.; Kellner, M. *Electrochem. Solid State Let.* **2007**, *10*, B19–B22.
(6) Gürsel, S. A.; Gubler, L.; Gupta, B.; Scherer, G. G. *Adv. Polym. Sci.* **2008**, *215*, 157–217.
(7) Li, L. F.; Deng, B.; Ji, Y. L.; Yu, Y.; Xie, L. D.; Li, J. Y.; Lu, X. F. *J. Membr. Sci.* **2010**, *346*, 113–120.
(8) Hickner, M. A.; Ghassemi, H.; Kim, Y. S.; Einsla, B. R.; McGrath, J. E. *Chem. Rev.* **2004**, *104*, 4587–4612.
(9) Kreuer, K. D. *J. Membr. Sci.* **2001**, *185*, 29–39.
(10) Rikukawa, M.; Sanui, K. *Prog. Polym. Sci.* **2000**, *25*, 1463–1502.
(11) Kerres, J. A. *J. Membr. Sci.* **2001**, *185*, 3–27.
(12) Jones, D. J.; Rozière, J. *Annu. Rev. Mater. Res.* **2003**, *33*, 503–555.
(13) Muldoon, J.; Lin, J.; Wycisk, R.; Takeuchi, N.; Hamaguchi, H.; Saito, T.; Hase, K.; Stewart, F. F.; Pintauro, P. N. *Fuel Cells* **2009**, *9*, 518–521.
(14) Tang, H.; Pintauro, P. N. *J. Appl. Polym. Sci.* **2001**, *79*, 49–59.
(15) Lee, C. H.; Lee, S. Y.; Lee, Y. M.; Lee, S. Y.; Rhim, J. W.; Lane, O.; McGrath, J. E. *ACS Appl. Mater. Interfaces* **2009**, *1* (5), 1113–1121.
(16) Bae, B.; Miyatake, K.; Watanabe, M. *ACS Appl. Mater. Interfaces* **2009**, *1* (6), 1279–1286.
(17) Lafitte, B.; Jannasch, P. *Adv. Funct. Mater.* **2007**, *17*, 2823–2834.
(18) Liu, B. J.; Robertson, G. P.; Kim, D. S.; Guiver, M. D.; Hu, W.; Jiang, Z. H. *Macromolecules* **2007**, *40*, 1934–1944.
(19) Gil, M.; Ji, X.; Li, X.; Na, H.; Hampsey, J. E.; Lu, Y. *J. Membr. Sci.* **2004**, *234*, 75–81.
(20) Tian, S. H.; Meng, Y. Z.; Hay, A. S. *Macromolecules* **2009**, *42*, 1153–1160.
(21) Xiao, G. Y.; Sun, G. M.; Yan, D. Y. *Abstr. Pap. Am. Chem. Soc.* **2003**, *225*, U558–U558.
(22) Bai, Z. W.; Shumaker, J. A.; Houtz, M. D.; Mirau, P. A.; Dang, T. D. *Polymer* **2009**, *50*, 1463–1469.
(23) Fang, J. H.; Guo, X. X.; Harada, S.; Watari, T.; Tanaka, K.; Kita, H.; Okamoto, K. *Macromolecules* **2002**, *35*, 9022–9028.
(24) Li, N. W.; Zhang, S. B.; Liu, J.; Zhang, F. *Macromolecules* **2008**, *41*, 4165–4172.
(25) Marestin, C.; Gebel, G.; Diat, O.; Mercier, R. *Adv. Polym. Sci.* **2008**, *216*, 185–258.
(26) Allcock, H. R.; Wood, R. M. *J. Polym. Sci., Polym. Phys.* **2006**, *44*, 2358–2368.
(27) Wycisk, R.; Pintauro, P. N. *Adv. Polym. Sci.* **2008**, *216*, 157–183.
(28) Staiti, P.; Lufrano, F.; Arico, A. S.; Passalacqua, E.; Antonucci, V. *J. Membr. Sci.* **2001**, *188*, 71–78.
(29) Peron, J.; Ruiz, E.; Jones, D. J.; Rozière, J. *J. Membr. Sci.* **2008**, *314*, 247–256.
(30) Mader, J.; Xiao, L. X.; Schmidt, T. J.; Benicewicz, B. C. *Adv. Polym. Sci.* **2008**, *216*, 63–124.
(31) Kang, S.; Zhang, C. J.; Xiao, G. Y.; Yan, D. Y.; Sun, G. M. *J. Membr. Sci.* **2009**, *334*, 91–100.
(32) Tan, N.; Xiao, G. Y.; Yan, D. Y. *Chem. Mater.* **2010**, *22*, 1022–1031.
(33) Shobha, H. K.; Smalley, G. R.; Sankarapandian, M.; McGrath, J. E. *Polym. Prepr.* **2000**, *41*, 180–181.
(34) Ma, X. H.; Zhang, C. J.; Xiao, G. Y.; Yan, D. Y.; Sun, G. M. *J. Polym. Sci., Polym. Chem.* **2008**, *46*, 1758–1769.
(35) Ma, X. H.; Shen, L. P.; Zhang, C. J.; Xiao, G. Y.; Yan, D. Y.; Sun, G. M. *J. Membr. Sci.* **2008**, *310*, 303–311.
(36) Zhang, C. J.; Kang, S.; Ma, X. H.; Xiao, G. Y.; Yan, D. Y. *J. Membr. Sci.* **2009**, *329*, 99–105.
(37) Ma, X. H.; Zhang, C. J.; Xiao, G. Y.; Yan, D. Y. *J. Power Sources* **2009**, *188*, 57–63.
(38) Gui, L. Y.; Zhang, C. J.; Kang, S.; Tan, N.; Xiao, G. Y.; Yan, D. Y. *Int. J. Hydrogen Energy* **2010**, *35*, 2436–2445.
(39) Kim, Y. S.; Einsla, B.; Sankir, M.; Harrison, W.; Pivovar, B. S. *Polymer* **2006**, *47*, 4026–4035.
(40) Yang, Y.; Siu, A.; Peckham, T. J.; Holdcroft, S. *Adv. Polym. Sci.* **2008**, *216*, 55–126.
(41) Lee, J. K.; Kerres, J. *J. Membr. Sci.* **2007**, *294*, 75–83.
(42) Xiao, G. Y.; Sun, G. M.; Yan, D. Y.; Zhu, P. F.; Tao, P. *Polymer* **2002**, *43*, 5335–5339.
(43) Whitaker, C. M.; Kott, K. L.; McMahon, R. J. *J. Org. Chem.* **1995**, *60*, 3499–3508.
(44) Smith JR, J. G.; Thompson, C. M.; Watson, K. A.; Connell, J. W. *High Perform. Polym.* **2002**, *14*, 225–239.
(45) Yu, X.; Roy, A.; Dunn, S.; Badami, A. S.; Yang, J.; Good, A. S.; McGrath, J. E. *J. Polym. Sci., Part A: Polym. Chem.* **2009**, *47*, 1038–1051.
(46) Kang, S.; Zhang, C. J.; Xiao, G. Y.; Yan, D. Y. *J. Funct. Polym.* **2009**, *22*, 199–202.
(47) Asano, N.; Aoki, M.; Suzuki, S.; Miyatake, K.; Uchida, H.; Watanabe, M. *J. Am. Chem. Soc.* **2006**, *128*, 1762–1769.
(48) Nasef, M. M.; Saidi, H.; Nor, H. M.; Foo, O. M. *J. Appl. Polym. Sci.* **2000**, *76*, 1–11.
(49) Roustan, J. L.; Ansari, N.; Lee, F.; Charland, J. P. *Inorg. Chim. Acta* **1989**, *155* (1), 11–12.
(50) Valle, G.; Casotto, G.; Zanonato, P. L.; Zarli, B. *Polyhedron* **1986**, *5* (12), 2093–2096.
(51) Wang, F.; Hickner, M.; Kim, Y. S.; Zawodzinski, T. A.; McGrath, J. E. *J. Membr. Sci.* **2002**, *197*, 231–242.
(52) Kim, Y. S.; Hickner, M. A.; Dong, L. M.; Pivovar, B. S.; McGrath, J. E. *J. Membr. Sci.* **2004**, *243*, 317–326.
(53) Zhang, H. Q.; Li, X. F.; Zhao, C. J.; Fu, T. Z.; Shi, Y. H.; Na, H. *J. Membr. Sci.* **2008**, *308*, 66–74.
(54) Roy, A.; Hickner, M. A.; Yu, X.; Li, Y. X.; Glass, T. E.; McGrath, J. E. *J. Polym. Sci., Part B: Polym. Phys.* **2006**, *44*, 2226–2239.

AM1000739